

Spin interference and the Fano effect in electron transport through a mesoscopic ring side-coupled with a quantum dot

This article has been downloaded from IOPscience. Please scroll down to see the full text article.

2010 J. Phys.: Condens. Matter 22 135301

(<http://iopscience.iop.org/0953-8984/22/13/135301>)

View [the table of contents for this issue](#), or go to the [journal homepage](#) for more

Download details:

IP Address: 129.252.86.83

The article was downloaded on 30/05/2010 at 07:41

Please note that [terms and conditions apply](#).

Spin interference and the Fano effect in electron transport through a mesoscopic ring side-coupled with a quantum dot

Guo-Hui Ding and Bing Dong

Department of Physics, Shanghai Jiao Tong University, Shanghai 200240,
People's Republic of China

Received 15 January 2010, in final form 19 February 2010

Published 12 March 2010

Online at stacks.iop.org/JPhysCM/22/135301

Abstract

We investigate the electron transport through a mesoscopic ring side-coupled with a quantum dot (QD) in the presence of Rashba spin-orbit (SO) interaction. It is shown that both the Fano resonance and the spin interference effects play important roles in the electron transport properties. As the QD level is around the Fermi energy, the total conductance shows a typical Fano resonance line shape. By applying an electrical gate voltage to the QD, the total transmission through the system can be strongly modulated. By threading the mesoscopic ring with a magnetic flux, the time-reversal symmetry of the system is broken, and a spin polarized current can be obtained even though the incident current is unpolarized.

1. Introduction

Spin related transport in semiconductor systems has attracted great interest in the field of spintronics [1], in which a variety of efforts are devoted to using the electron spin instead of the electron charge for information processing or even quantum information processing. Several interesting spintronic devices have been proposed, the most prominent one is the Datta–Das spin field effect transistor (SFET) [2]. This proposal uses the Rashba SO coupling [3] to perform the controlled rotations of the spin of electron. Although the SFET has not yet been realized in experiment, it has been demonstrated in experiments that the strength of the SO interaction is quite tunable by an external electric field or gate voltage, which gives the SFET a promising future [4].

The quantum coherence of an electron is preserved when it is transported through a system of mesoscopic scale. This has been manifested explicitly in the conductance AB oscillation through the Aharonov–Bohm (AB) interferometer [5], where an electrical charge circles around the magnetic flux enclosed by the AB ring and acquires an AB phase. In the presence of Rashba SO coupling, aside from the AB effect, another important Berry phase effect called the Aharonov–Casher (AC) effect [6] occurs, it is due to the electron magnetic moment moving in an effective magnetic field caused by the Rashba SO coupling. Recently, the AC effect has been observed experimentally in electron transport through semiconductor mesoscopic rings [7–11]. The modulation of the conductance

can be explained theoretically in terms of noninteracting electrons [9, 12, 13]. The electron interaction effect on conductance in this Rashba SO coupling ring has also been studied based on the Hubbard model [14].

The electron transport through a AB ring with a QD embedded in one arm of the ring is another interesting topic, and has been studied extensively both in theory and experiments [15–17]. In this case, the Coulomb repulsive interaction in the QD has to be taken into account. When Rashba SO interaction is presented inside the QD, it is predicted theoretically that substantial spin polarized current or conductance can be induced by the combined effect of the Rashba SO interaction and the magnetic flux threading the ring [15]. A flux-tunable resonant tunneling diode has been proposed recently in the system with a ring subject to a Rashba SO interaction [18]. In these AB ring-QD systems, the important interference effect known as the Fano resonance emerges. For electron transport through a quantum wire with side branches, defect levels or one-dimensional rings, the Fano effect is manifested as antiresonances in the electron transmission coefficient [19–21]. It is also pointed out in [22, 23] that phase fluctuations due to this kind of antiresonance can be an important road to the emergence of decoherence. At present, the Fano effect is known to be an ubiquitous phenomenon observed in a large variety of systems. One important progress in recent years is the observation of the Fano resonances in various condensed matter systems, including an impurity atom on a metal surface [24], a

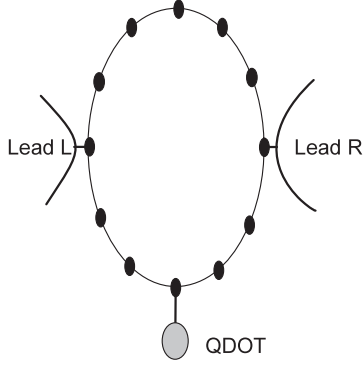


Figure 1. Schematic diagram for the lattice model of a two terminal AB ring side-coupled with a quantum dot.

single-electron transistor [25, 26], a quantum dot in an AB interferometer [17], etc.

In this paper we will investigate the electron transport properties through a AB ring side-coupled with a QD, and in the presence of Rashba SO interaction in the ring. The geometry of this system is plotted schematically in figure 1. This kind of geometry has been realized in experiment, and the Fano resonances in electron transport through the ring have been observed [27]. However, the SO coupling effects in this system have not been well investigated. In this paper we shall present our study on the effects of the Rashba SO coupling on the Fano resonance and the spin interference effects. It is shown that the interplay of the spin interference and the Fano effect greatly influence the electron transport properties in this system.

2. Mesoscopic ring side-coupled with a quantum dot

The electrons in a closed ring with SO coupling of the Rashba term can be described by the following Hamiltonian in polar coordinates [28, 29]

$$H_{\text{ring}} = \Delta \left(-i \frac{\partial}{\partial \varphi} + \phi \right)^2 + \frac{\alpha_R}{2} \left[(\sigma_x \cos \varphi + \sigma_y \sin \varphi) \left(-i \frac{\partial}{\partial \varphi} + \phi \right) + \text{H.c.} \right], \quad (1)$$

where $\Delta = \hbar^2 / (2m^* R^2)$, R is the radius of the ring. α_R will characterize the strength of the Rashba SO interaction. $\phi = \Phi / \Phi_0$, with Φ being the external magnetic flux enclosed by the ring, and $\Phi_0 = 2\pi \hbar c / e$ is the flux quantum.

One can rewrite the above 1D Hamiltonian in terms of a lattice model in the spatial space [30].

$$H_{\text{ring}} = - \sum_{n=1}^{N_R} [t_{\varphi}^{n,n+1;\sigma,\sigma'} c_{n,\sigma}^{\dagger} c_{n+1,\sigma'} + \text{H.c.}], \quad (2)$$

where $n = 1, 2, \dots, N_R$ is the lattice site index along the azimuthal (φ) direction, with N_R being the total number of the lattice sites, and we assume $N_R = 4N$.

$$\hat{t}_{\varphi}^{n,n+1} = [t_0 \hat{I}_s - it_{\text{so}} (\sigma_x \cos \varphi_{n,n+1} + \sigma_y \sin \varphi_{n,n+1})] e^{i2\pi\phi/N_R}. \quad (3)$$

Here $\varphi_{n,n+1} \equiv (\varphi_n + \varphi_{n+1})/2$ with $\varphi_n \equiv 2\pi(n-1)/N_R$, $t_0 \equiv \hbar^2/2m^*a^2$ with a being the lattice spacing. $t_{\text{so}} \equiv \alpha_R/2a$ is the SO hopping parameter in this lattice model, and \hat{I}_s is the 2×2 identity matrix. One can introduce a dimensionless parameter $Q_R \equiv \alpha_R/R\Delta = (t_{\text{so}}/t_0)N_R/\pi$ to characterize the Rashba SO interaction strength [30].

Now we consider the system side-coupled with a QD, which can be described by the Anderson impurity model,

$$H_d = \sum_{\sigma} \epsilon_d d_{\sigma}^{\dagger} d_{\sigma} + U n_{d\uparrow} n_{d\downarrow}, \quad (4)$$

where ϵ_d is the energy level of QD, and U is the on-site Coulomb interaction. The tunneling between the dot level and the ring is given by

$$H_{d\text{-ring}} = t_D \sum_{\sigma} (d_{\sigma}^{\dagger} c_{N+1,\sigma} + \text{H.c.}). \quad (5)$$

The ring is also connected to the left and right leads with the Hamiltonian

$$H_{\text{lead}} = \sum_{k,\eta,\sigma} \epsilon_{k\eta} a_{k\eta\sigma}^{\dagger} a_{k\eta\sigma}, \quad (6)$$

where $\eta = L, R$. The tunneling Hamiltonian between the leads and the ring is given as

$$H_{\text{lead-ring}} = \sum_{k,\sigma} v_{kL} [a_{kL\sigma}^{\dagger} c_{1,\sigma} + \text{H.c.}] + \sum_{k,\sigma} v_{kR} [a_{kR\sigma}^{\dagger} c_{2N+1,\sigma} + \text{H.c.}]. \quad (7)$$

It should be noted that in this lattice model the electrons from the left and right leads only have nonzero tunneling amplitudes to the ring sites 1 and $2N+1$, respectively. The hybridization strength between the lead η and the ring can be defined as $\Gamma^{\eta} = 2\pi \sum_k |v_{k\eta}|^2 \delta(\omega - \epsilon_{k\eta})$

Thereby, the total Hamiltonian for the system should be

$$H = H_{\text{lead}} + H_{\text{ring}} + H_d + H_{d\text{-ring}} + H_{\text{lead-ring}}. \quad (8)$$

By the equation of motion method, one can obtain a set of coupled equations for the retarded Green's functions (GFs) of the QD $G_{d\sigma}^r$ and that of the ring $G_{i\sigma,j\sigma'}^r$. However due to the on-site Coulomb interaction, this set of equations cannot be solved exactly. We will consider the QD in the Coulomb blockade regime. In order to treat the strong on-site Coulomb interaction in the dot level, we use the self-consistent decoupling procedure proposed by Hubbard [31], in which the low energy excitations involved in the Kondo effect are neglected, but it can properly describe the Coulomb blockade effect. Hence it is believed to be a good approximation for temperature higher than the Kondo temperature T_K . Within this approximation, the equations of motion for the GFs have the same structure as those of the noninteracting system, except that now the bare Green function of the QD is replaced by

$$g_{d\sigma}^r(\omega) = \frac{1 - \langle n_{d\bar{\sigma}} \rangle}{\omega - \epsilon_d + i0^+} + \frac{\langle n_{d\bar{\sigma}} \rangle}{\omega - \epsilon_d - U + i0^+}. \quad (9)$$

Then we can obtain all retarded GFs conveniently by writing the Hamiltonian in the matrix form, and numerically invert the

matrix [23]. As the final step, the dot occupation number $\langle n_{d\bar{\sigma}} \rangle$ is determined by the self-consistent equation

$$\langle n_{d\bar{\sigma}} \rangle = - \int \frac{d\omega}{\pi} n_F(\omega) \text{Im} G_{d\bar{\sigma}}^r(\omega), \quad (10)$$

where $n_F(\omega)$ is the Fermi–Dirac distribution function.

For the electron transport through this system, the spin-resolved conductance at zero temperature will be given by the transmission probability at the Fermi energy $G_{\sigma\sigma'} \equiv T^{\sigma\sigma'}(\omega = E_F)$, with the generalized Landauer formula [32]

$$T^{\sigma\sigma'}(\omega) = \text{Tr}[\hat{\Gamma}_L^\sigma \hat{G}^r \hat{\Gamma}_R^{\sigma'} \hat{G}^a]. \quad (11)$$

3. Results and discussions

In this section we will present the numerical results of our calculation. We consider a quantum ring with radius $R = 100$ nm, and the effect mass $m^* = 0.04m_e$, where m_e is the free electron mass. One can obtain the energy scale $\Delta \approx 0.1$ meV. For a typical experimentally accessible Rashba strength $\alpha_R = 1 \times 10^{-11}$ eV m, one has the parameter $\alpha_R/a \approx \Delta$, therefore the dimensionless Rashba SO parameter $Q_R = \alpha_R/R\Delta \approx 1$. In our calculation, we will take the bandwidth parameters $t_0 = 1$ as the energy unit, the parameter $t_D = 0.3$, $U = 1.0$, the total number of ring lattice sites $N_R = 40$ and the Fermi energy $E_F = -0.52$.

In figure 2(a) the linear conductance versus the QD level ϵ_d is plotted at zero magnetic flux ($\phi = 0$), but with different SO coupling strength ($Q_R = 0.0, 1.0, 1.5$). Without the Rashba SO coupling ($Q_R = 0$), one can see that the curve is dominated by two peaks around $\epsilon_d - E_F \approx 0$ and $-U$. The peaks show typical asymmetric Fano resonance line shapes due to the interference of the electron passing through the quasi-continuous states in the ring and the discrete state in the QD. This kind of antiresonance is also observed in electron transport through a quantum wire with side branches [19], defect levels [21] or one-dimensional disordered rings [20]. It is noticed that the Rashba SO interaction can strongly affect the Fano resonance in this system. By increasing the Rashba SO interaction Q_R , the Fano line shape changes drastically, for example, the Fano resonance with $Q_R = 1.5$ has an opposite Fano factor to the $Q_R = 0.0, 1.0$ cases. In order to better understand the electron transport through the ring, we plot the transmission probability $T(\omega)$ versus the incident electron energy in figure 2(b). The quasi-periodic peaks in $T(\omega)$ correspond to the energy levels in the quantum ring. Since we assume the QD level ϵ_d is below the Fermi energy in the calculation, the QD is occupied by one electron, hence antiresonances are observed in the transmission probability for an electron with incident energy $\omega \approx \epsilon_d + U$. There are also other antiresonances in the transmission probability, as shown in figure 2(b), we will attribute them to the fact the ring is coupled with the leads. For the system with large bias voltage between leads, multi-levels in the ring are involved in the electron conduction [33], therefore one may expect that the energy dependent transmission probability in the energy range between left and right chemical potentials is essential to the out of equilibrium transport properties of this system. However,

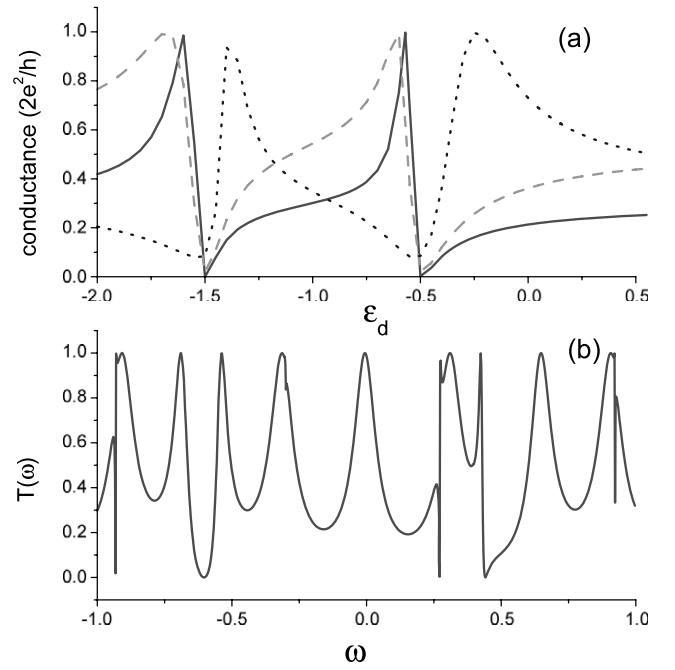


Figure 2. (a) The total conductance through the 1D ring versus the QD level ϵ_d for the Rashba SO interaction parameter $Q_R = 0.0$ (solid line), 1.0 (dashed line), and 1.5 (dotted line), respectively. (b) The transmission probability $T(\omega)$ versus the incident electron energy for the system with quantum dot level $\epsilon_d = -6.0$, $Q_R = 0.0$. The other model parameters are taken as $t_0 = 1.0$, $t_D = 0.5$, $U = 1.0$, $E_F = -0.52$, and $\phi = 0$.

we shall focus our attention on the linear response regime in the present paper.

Next, we consider the conductance versus Rashba SO coupling strength for three different values of QD level $\epsilon_d = -0.4, -0.55, -0.6$, the results are shown in figure 3. For the system with SO coupling but without external magnetic flux, it still has the time-reversal symmetry. We find the spin-resolved conductances have the symmetry $G_{\uparrow} = G_{\downarrow}$, therefore only G_{\uparrow} is plotted. In the presence of SO interaction, the conductance shows quasi-periodical oscillations with the value of Q_R as the result of the interference effect for electron transport through the ring. Both the non-spin-flip $G_{\uparrow\uparrow}$ conductance and the spin-flip conductance $G_{\uparrow\downarrow}$ can reach zero at some particular values of Q_R . In this case, totally destructive interference of this kind of spin-resolved electron transport is achieved. It is noticed that at some value of Q_R , the spin non-flip conductance $G_{\uparrow\uparrow}$ is zero, but with a finite spin-flip conductance $G_{\uparrow\downarrow}$, therefore the ring-dot system can act as a spin-flip device. Since, the non-spin-flip and spin-flip conductance obtain zero values at different position of Q_R , there are always some leakage currents in this system. It is also observed that the conductance can be strongly modulated by the QD level, it can change from a local maximum to a local minimum at the same value of SO coupling Q_R .

In figure 4 we give the flux dependence of the linear conductance at different values of Q_R . The conductance is a periodic function of the enclosed magnetic flux ϕ . Without SO coupling, the conductance is independent of the electron spin. In the presence both of SO interaction and magnetic

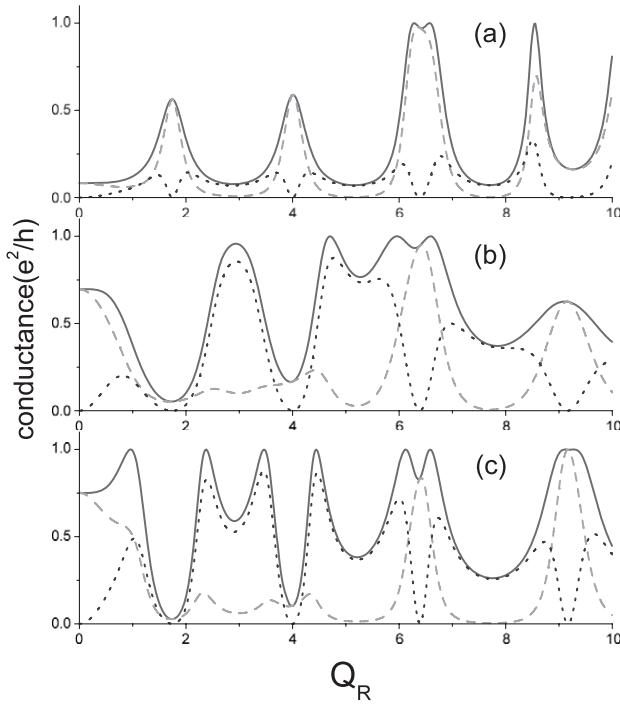


Figure 3. The spin-resolved conductance versus Rashba SO interaction parameter for different values of dot energy level: (a) $\epsilon_d = -0.4$; (b) $\epsilon_d = -0.55$, and (c) $\epsilon_d = -0.6$. The non-spin-flip conductance $G_{\uparrow\uparrow}$, the spin-flip conductance $G_{\uparrow\downarrow}$ and the spin-resolved conductance $G_{\uparrow} = G_{\uparrow\uparrow} + G_{\uparrow\downarrow}$ are plotted as a dashed line, dotted line and solid line, respectively. The other parameters are the same as those of figure 1.

flux, the time-reversal symmetry of this system is broken, and the result shows the spin-resolved conductances are spin dependent ($G_{\uparrow} \neq G_{\downarrow}$). By increasing the SO coupling strength Q_R , the line shapes of conductances do not change significantly, but it is easy to observe that the conductance line shapes are shifted along the ϕ axis. This can be interpreted as that in the presence of SO coupling, the electron acquires a spin Berry phase when transported through the ring, which will act as an effective magnetic flux in the electron conductance. Since the conductance lines G_{\uparrow} and G_{\downarrow} shift differently, it indicates that the spin Berry phases are different for spin up and spin down incident electrons.

From the above result, one can see that it is possible to obtain a spin polarized current even when the incident electron is spin unpolarized. In the linear response regime, we define the current spin polarization $\eta = (G_{\uparrow} - G_{\downarrow}) / (G_{\uparrow} + G_{\downarrow})$. For different values of SO coupling parameter Q_R , the calculated current polarization η versus the magnetic flux ϕ is plotted in figure 5. It is observed that the spin polarization can achieve a value of $\eta \approx 50\%$ at some particular SO coupling strength Q_R and enclosed magnetic flux ϕ . It is interesting to notice that at zero bias voltage, although there are no net charge and spin currents between the left and right leads, finite charge and spin currents circling around the ring can exist when the ring is threaded by a magnetic flux [34]. It is also noted that when the QD in this system is driven by a time dependent gate, even at zero bias a charge or spin current might be observed due to the quantum pumping phenomena [35].

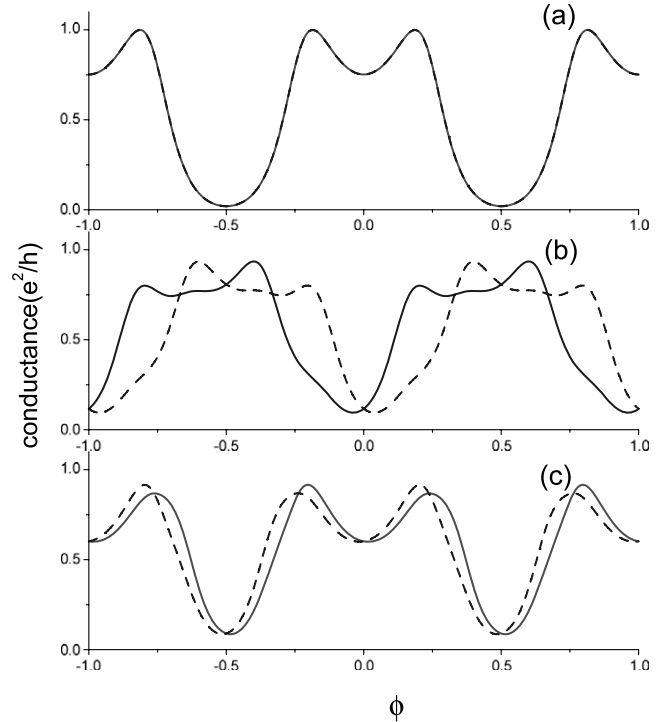


Figure 4. The spin-resolved conductance G_{\uparrow} (solid line), and G_{\downarrow} (dashed line) versus the threading magnetic flux ϕ for several Rashba SO interaction parameters: (a) $Q_R = 0.0$; (b) $Q_R = 1.5$; (c) $Q_R = 3.0$. The dot level is fixed at $\epsilon_d = -0.6$, and the other parameters are the same as those of figure 1.

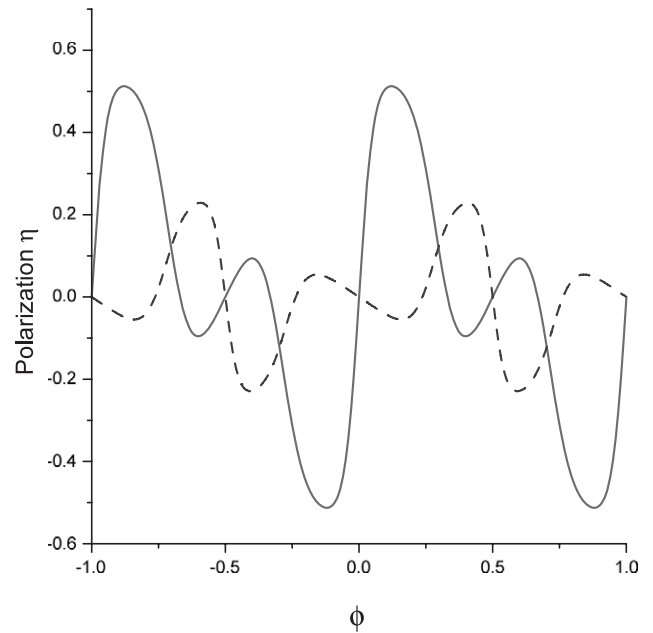


Figure 5. The spin polarization η versus the threading magnetic flux ϕ with Rashba SO interaction parameters: $Q_R = 1.5$ (solid line); $Q_R = 3.0$ (dashed line). The dot level is fixed at $\epsilon_d = -0.6$, and the other parameters are the same as those of figure 1.

4. Conclusions

In summary, we have investigated the Rashba SO coupling effect on the electron transport through an AB interferometer

with one arm side-coupled with a QD. It is shown that in the presence of a QD, the Fano effect will play a significant role in the electron transmission through the AB ring, therefore, by tuning the QD energy level, we can modulate the total conductance of the system. In the presence of Rashba SO interaction in the mesoscopic ring, the electron spin can be reversed at some particular value of Q_R . With nonzero magnetic flux ϕ enclosed, the time-reversal symmetry of the system is broken, one can obtain a partially spin polarized current after the electron transport through this AB ring, even though the incident electron is not spin polarized. The current spin polarization can be tuned by QD gate voltage, magnetic flux and the Rashba interaction strength. One may expect further experiment on semiconductor mesoscopic rings with Rashba SO interaction could reveal more interesting spin interference and Fano resonance effects.

Acknowledgments

This project is supported by the National Natural Science Foundation of China, the Shanghai Pujiang Program, and the Program for New Century Excellent Talents in University (NCET).

References

- [1] Zutic I, Fabian J and Das Sarma S 2004 *Rev. Mod. Phys.* **76** 323
- [2] Datta S and Das B 1990 *Appl. Phys. Lett.* **56** 665
- [3] Bychov Y A and Rashba E I 1984 *J. Phys. C: Solid State Phys.* **17** 6039
- [4] Nitta J, Akazaki T, Takayanagi H and Enoki T 1997 *Phys. Rev. Lett.* **78** 1335
- [5] Webb R A, Washburn S, Umbach C P and Laibowitz R B 1985 *Phys. Rev. Lett.* **54** 2696
- [6] Aharonov Y and Casher A 1984 *Phys. Rev. Lett.* **53** 319
- [7] Morpurgo A F, Heida J P, Klapwijk T M, van Wees B J and Borghs G 1998 *Phys. Rev. Lett.* **80** 1050
- [8] Yau J B, De Poortere E P and Shayegan M 2002 *Phys. Rev. Lett.* **88** 146801
- [9] König M, Tschetschetkin A, Hankiewicz E M, Sinova J, Hock V, Daumer V, Schäfer M, Becker C R, Buhmann H and Molenkamp L W 2006 *Phys. Rev. Lett.* **96** 076804
- [10] Bergsten T, Kobayashi T, Sekine Y and Nitta J 2006 *Phys. Rev. Lett.* **97** 196803
- [11] Grbić B, Leturcq R, Ihn T, Ensslin K, Reuter D and Wieck A D 2007 *Phys. Rev. Lett.* **99** 176803
- [12] Frustaglia D and Richter K 2004 *Phys. Rev. B* **69** 235310
- [13] Wang M and Chang K 2008 *Phys. Rev. B* **77** 125330
- [14] Lobos A M and Aligia A A 2008 *Phys. Rev. Lett.* **100** 016803
- [15] Sun Q F, Wang J and Guo H 2005 *Phys. Rev. B* **71** 165310
Sun Q F and Xie X C 2006 *Phys. Rev. B* **73** 235301
- [16] Heary R J, Han J E and Zhu L Y 2008 *Phys. Rev. B* **77** 115132
- [17] Kobayashi K, Aikawa H, Katsumoto S and Iye Y 2002 *Phys. Rev. Lett.* **88** 256806
Kobayashi K, Aikawa H, Katsumoto S and Iye Y 2003 *Phys. Rev. B* **68** 235304
Kobayashi K, Aikawa H, Sano A, Katsumoto S and Iye Y 2004 *Phys. Rev. B* **70** 035319
- [18] Citro R and Romeo F 2008 *Phys. Rev. B* **77** 193309
- [19] Guinea F and Verges J A 1987 *Phys. Rev. B* **35** 979
- [20] D'Amato J L, Pastawski H M and Weisz J F 1989 *Phys. Rev. B* **39** 3554
- [21] Wang X R, Wang Y P and Sun Z Z 2002 *Phys. Rev. B* **65** 193402
- [22] Foa Torres L E F, Pastawski H M and Medina E 2006 *Europhys. Lett.* **73** 164
- [23] Pastawski H M, Foa Torres L E F and Medina E 2002 *Chem. Phys.* **281** 257
- [24] Madhavan V, Chen W, Jamneala T, Crommie M F and Wingreen N S 1998 *Science* **280** 567
- [25] Göres J, Goldhaber-Gordon D, Heemeyer S, Kastner M A, Shtrikman H, Mahalu D and Meirav U 2000 *Phys. Rev. B* **62** 2188
Zacharia I G, Goldhaber-Gordon D, Granger G, Kastner M A, Khavin Y B, Shtrikman H, Mahalu D and Meirav U 2001 *Phys. Rev. B* **64** 155311
- [26] Johnson A C, Marcus C M, Hanson M P and Gossard A C 2004 *Phys. Rev. Lett.* **93** 106803
- [27] Fuhrer A, Brusheim P, Ihn T, Sigrist M, Ensslin K, Wegscheider W and Bichler M 2006 *Phys. Rev. B* **73** 205326
- [28] Meijer F E, Morpurgo A F and Klapwijk T M 2002 *Phys. Rev. B* **66** 033107
- [29] Spletstoesser J, Governale M and Zülicke U 2003 *Phys. Rev. B* **68** 165341
- [30] Souma S and Nikolić B K 2004 *Phys. Rev. B* **70** 195346
Nikolić B K and Souma S 2005 *Phys. Rev. B* **71** 195328
- [31] Hubbard J 1963 *Proc. R. Soc. A* **276** 238
- [32] Meir Y, Wingreen N S and Lee P A 1993 *Phys. Rev. Lett.* **70** 2601
- [33] Wang S D, Sun Z Z, Cue N, Xu H Q and Wang X R 2002 *Phys. Rev. B* **65** 125307
- [34] Ding G H and Dong B 2007 *Phys. Rev. B* **76** 125301
- [35] Foa Torres L E F 2005 *Phys. Rev. B* **72** 245339